Influence of Epoxidized Natural Rubber of the thermoformability of Poly(Lactic Acid) biopolymer films using elevated temperature ball burst tests

T. Tábi[1,2] · **D. Gere**[1] · **G. Csézi**[1] · **K. Pölöskei**[1]

Abstract

In this paper, we investigated the thermoformability of Epoxidized Natural Rubber (ENR)-filled Poly(Lactic Acid) (PLA) films using elevated temperature tensile and ball burst tests. Three different D-Lactide contents of PLA were used to be able to analyze the effect of crystallization and crystallinity. We observed that the ENR acted as a nucleating agent in PLA when the blend was cooled from melt or cold crystallized, but it retarded the drawing-induced crystallization of PLA at elevated temperature tensile testing since ENR droplets acted as obstacles. The effect of NR on PLA crystallization was also found to be dependent on D-Lactide content. In the ball burst test, different behaviors were observed for PLA with the lowest D-Lactide content, which was caused by the complex stress state that even more induced crystallization of PLA and then a single-axis tensile test.

Introduction

From the beginning of the twenty-first century, the biopolymers got more and more focus due to their two exceptional properties; namely, they can be produced using renewable agricultural biomass, and they are inherently biodegradable. Accordingly, it is believed that they could solve or at least reduce the plastic industry's dependence on petroleum, and furthermore, due to their biodegradability, the accumulation of single-use plastics in landfills can be reduced. Due to these two exceptional properties, biopolymers fulfill the concept of environmental consciousness and circular economy as well as fit into nature's life cycle [1–5].

There are currently around a dozen types of biopolymers in the market, but the most available and promising one is Poly(Lactic Acid) (PLA). PLA is a semi-crystalline, thermoplastic, aliphatic polyester, and to produce it, first the glucose content of starch- or sugar-containing crops like wheat, maize, potato, rice, or sugar beet, respectively, is fermented into Lactic Acid (LA). From LA usually first its dimer is made called Lactide, and afterward, PLA is synthetized from Lactide through ring opening polymerization (ROP). Due to the fact that LA has two stereoisomers named L-Lactic Acid (LLA) and D-Lactic Acid (DLA), three Lactide variations exist of L-Lactide, D-Lactide and D-L-Lactide (also known as meso-Lactide). Accordingly, PLA is actually not one but a whole polymer family, since it can be considered as the copolymer of D- and L-Lactide. In nature, the existence of L-Lactide is more favorable; thus, a conventional PLA grade contains mainly L-Lactide with around 1–15% of D-Lactide content, while Poly(L-Lactic Acid) (PLLA) and Poly(D-Lactic Acid) (PDLA) are isotactic PLA grades that contain 0% and 100% D-Lactide, respectively [6].

D-Lactide content significantly affects the thermal, crystallization and mechanical properties, namely lower D-Lactide content, and thus, purer PLA grade represents higher crystal melt temperature and faster crystallization; thus, naturally PLLA has the highest crystal melt temperature of around 175 °C. Even though PLLA has the fastest crystallization rate due to its isotactic structure compared

✉ T. Tábi
tabi@pt.bme.hu

1 Department of Polymer Engineering, Faculty of Mechanical Engineering, Budapest University of Technology and Economics, Muegyetem Rkp. 3., Budapest 1111, Hungary

2 ELKH–BME Research Group for Composite Science and Technology, Muegyetem Rkp. 3., Budapest 1111, Hungary

to higher D-Lactide content PLA grades, during processing, even PLLA products will become mostly transparent and will have low crystallinity due to the still slower crystallization rate compared to ordinary plastics like Poly(Ethylene) (PE) or Poly(Propylene) (PP) [7, 8]. PLA can be processed using normal/traditional plastic processing machines like injection molding, thermoforming, extrusion, bottle or film blowing or fused deposition modeling (FDM) [9, 10]. A PLA product typically represents high modulus (~3 GPa tensile modulus) and strength (~65 MPa tensile strength), but it is brittle with 3–5% of strain at break and 2–4 kJ m^{-2} of Charpy impact strength [7]; however, it can be widely modified by, for example, using reinforcements [11] or other polymers including thermoplastic starch (TPS) [12] or poly(3-hydroxybutyrate-co-3-hydroxyvalerate) (PHBV) [13, 14].

Regarding crystallization, PLA crystallizes slowly and it has several crystal forms: α, β, γ and η (also called stereocomplex) [15]. α form is the most common type forms during processing of PLA (either during cooling from melt or solid state crystallization/ annealing) or from solution [16, 17]. A less ordered crystal form of α' also exists with the same conformation but a loose packing manner compared to the more ordered α form [18–20]. β form develops through the high drawing of the α form at a high temperature [21, 22], while γ crystal is formed by applying epitaxial crystallization [23]. Finally, if the optically pure PLLA and PDLA are blended, stereocomplex PLA forms [24–26]. Naturally, the crystal structure formed has major influence on the thermomechanical properties of the product and even there is high difference in properties due to α or α' crystal structure [27].

In a lot of cases, it is aimed to use PLA for the substitution of ordinary plastics in case of thermoformed products, but to do so, its toughness should be improved. One of the easiest possibilities for improving impact strength or ductility of PLA is to add another biobased material, which is ductile in nature. A possible biomaterial is the cis-1,4-Poly(isoprene). It is the main component in both Natural Rubber (NR) and Isoprene Rubber (IR) [28]. Nowadays, NR is considered as one of the major components in the rubber industry, while synthetic rubbers (SRs) are used to replace NR. Latex can be obtained by tapping the Hevea brasiliensis, also called as "rubber-tree". Latex is considered as a water suspension of 30–38% cis-1,4-Poly(isoprene). Today, obtaining NR is still 99% based on the "rubber-tree" by solidifying the suspension. Before further processing, NR is an amorphous elastomer form and has a density around 0.93 g cm^{-3}. It has also low strength and stiffness, while being combustible. To obtain better properties, it is usually cross-linked (cured) or as it is called in the rubber industry, vulcanized, usually using sulfur. Based on the extent of curing, one can divide rubbers into soft and hard rubber [29].

The properties of NR, like biobased feature, biocompatibility, low Young's modulus, enormous toughness and low cost, make it perfectly suitable for toughening rigid polymers like PLA. Many papers deal with the investigation of NR-filled PLA blends [30–40].

Regarding the morphology of NR-filled PLA, a dispersed structure was found, where NR is the dispersed phase and PLA plays the role of the continuous phase (typical island-sea-type morphology), while there is weak adhesion found between the phases. In the research of Bitinis et al. [30], it was also found that the diameter of the dispersed NR droplets could be influenced by the processing parameters. Accordingly, increasing melt temperature and thus decreasing viscosity during processing cause an increase in the size of the NR droplets. For instance, using an internal mixer, an average droplet size of 1–2 μm could be achieved. Epoxidization of the NR (ENR) could also be an effective tool to achieve a finer size distribution (lower droplet size) as well as partial compatibility between the phases and overall improved strain and impact properties [31, 32]. In a research, 20 mass% and 35 mass% NR content PLA blends were investigated and it was observed that when the blend contained 35% of NR, the mechanical properties were superior; for example, seven times higher impact strength was achieved compared to pristine PLA. This was caused by an inter-penetrating network (IPN) of NR and PLA developed due to the right NR content [33]. This IPN structure or also called as co-continuous structure is highly advantageous to achieve high toughness properties, not only in the NR-filled PLA, but also in other bioplastic blends as well. In the research of Yuan et al. [34], dicumyl-peroxide cross-linking additive was applied to the blend. It was pointed that the 20 mass% NR and cross-linking agent-filled PLA blend improved the adhesion between the phases after vulcanization. Additionally, it was found that even at this low NR content, an IPN structure was found that increased the mechanical properties of the blend. Finally, the particle size of the NR droplets is also influenced by the NR content, since the increasing NR content increases their particle (droplet) size as well [35].

According to the crystallization of NR-filled PLA, it was demonstrated that the blending of NR and PLA improves the crystallization of PLA; thus, it a minor nucleating ability of NR on PLA was found and thus a small increase in the crystallinity of PLA could be measured [30, 31, 33–35]. At the same time, some papers reported the opposite; thus, the crystallization of PLA was retarded by the presence of NR [32, 36]. Most probably, the nucleation ability of NR on PLA is influenced by the purity (tacticity) of PLA used (D-Lactide content).

Regarding the mechanical properties of NR-filled PLA blends, it was observed that adding NR to PLA typically acts as a plasticizer; namely, strength and modulus is reduced, while elongation and toughness is improved, especially

when NR phase not only appeared as a dispersed but co-continuous phase. One optimal NR content was found around 10 mass% according to the crystallization, thermal stability and mechanical properties, in the investigated 0–30 mass% NR content range [30, 31, 33, 37, 38]. When using NR content above 20 mass%, the elongation was highly reduced, due to the large NR droplet size and to the coalescence of the droplets [35]. When ENR is used, it was pointed that it had higher adhesion with PLA; at the same time, the untreated NR-filled PLA blend reached better impact properties [37]. As a continuation of this research, the influence of the mastication of NR was also investigated. During this process, both molecular weight and viscosity decrease causing the particle size to decrease. Masticating NR causes an enormous increase in impact strength due to reaching the optimal NR droplet size of around 0.5–1 μm, while below this level, toughness decreases. In the studies of Yuan et al. [34, 35], 20 mass% and 40 mass% NR content PLA blends were investigated with vulcanization additive (dicumyl-peroxide). By using dynamic vulcanization, 35 mass% NR-filled PLA blends were developed with the outstanding ~ 60 kJ m^{-2} impact strength, while the impact strength of neat PLA was around only 3 kJ m^{-2} [34]. Furthermore, the same blend not only had high impact strength but also very high elongation at break (> 200%) [35].

According to the thermal stability, it was found that PLA/ENR blends have slightly improved thermal stability than PLA/NR blends due to the better interfacial adhesion [35].

The degradation properties of 90/10 mass% PLA/NR blend were investigated based on simulated compost according to ISO 20200 standard [39]. It was found that the PLA/NR blend needed more time for degradation compared to neat PLA, since the rather slow rate of degradation of NR reduced the overall rate of degradation of the whole blend. In our previous paper [40], a toughening mechanism was found, namely the combined use of NR followed by an annealing process causes a positive cross-effect. This means that the toughness of the NR-filled PLA blend had enormously higher toughness with annealing than without annealing. A similar phenomenon could also be seen in the paper of Suksut and Deeprasertkul [36], since they added nucleating agents to 10 mass% NR content PLA, where the tensile toughness of the nucleated and NR-filled PLA compounds was higher than the only nucleated or only NR-filled PLA compounds. However, in this case no direct connection between the crystallinity and the presence of NR on the toughness was found.

As it was found, NR is suitable for enhancing the strain and the ductility of PLA films or sheets used for thermoforming. However, currently, there is no direct measurement to determine and characterize the deformability and thermoformability of a plastic film. In most cases, elevated temperature tensile measurements directly performed thermoforming tests with the final molds, different burst tests [41], simulations [42], pneumatic tests (plastic film is heated up and pneumatically inflated) or the combination of the mentioned are used to examine the behavior of a polymer sheet during thermoforming. The ball burst test is originally designed for investigating fabrics. Typically, multiaxial deformation is caused by the penetration of the ball on the clamped fabric, and these conditions are much closer to the real multiaxial stress conditions of thermoforming. Accordingly, it is worth investigating the applicability of the ball burst test for thermoforming sheets. Thermoforming investigation of PLA sheets is a fairly new research field; therefore, in our latest publication [43] different purity (D-Lactide content) PLA films were analyzed regarding thermoformability by applying using ball burst tests at various rates of deformation and temperatures. It was found that during ball burst testing, the crystallinity significantly increased (from around 6% to 46–48% in case of low D-Lactide content PLA (1.4%) due to the joint effect of elevated temperature (above T_g) and mechanical stress. Both D-Lactide content, testing rate and testing temperature had an influence on the crystallinity.

Finally, since according to our previous results, on the one hand there is a toughening mechanisms, there is a synergistic effect between the presence of NR as toughening agent and the crystalline structure of PLA on the toughness of NR-filled PLA blends, and on the other hand, we found that during thermoforming or ball burst test the crystallinity of PLA significantly increases; thus, we found it worth to investigate the thermoformability properties of PLA/NR blends using elevated temperature tensile testing and ball burst tests, where the crystallinity needed to initiate the toughening mechanism could be developed by rubbery state strain.

Experimental

Materials and processing

NatureWorks (Minnetonka, MN, USA) PLA grades of 4032D, 2003D and 4060D were purchased and used for this research. The grades had a D-Lactide content of 1.4%, 4.3% and 12%, respectively. All the used PLA grades had 1.24 g cm^{-3} of density, 55–60 °C glass transition temperature, a melting point between 155 and 170 °C (the lower the D-Lactide content the higher the melting point) and an MFI of 6–7 g 10 min^{-1} (at 210 °C and 2.16 kg load). 6-h 80 °C drying was applied with a hot air drier to remove moisture. Epoxyprene 50 (Thailand) grade ENR from Mai Guthrie Public Company was used for the research. This ENR is produced using natural rubber latex with 50% epoxidation. Its T_g is − 24 °C, the density is 1.20 g cm^{-3}, while the Mooney viscosity 70–100.

A corotating double screw extruder type LabTech LTE 26–44 Scientific (Labtech Engineering Ltd., Samutpreken, Thailand) with an L/ᴅ = 44 and a screw diameter of 26 mm was used for compounding of PLA and ENR. Zone temperatures of the extruder were 175 and 190 °C between the hopper and the die, while the screw rotational speed was 10 rpm. 10 mass% ENR was added to PLA. After compounding and pelletizing, another drying sequence was used at 80 °C for 6 h to crystallize the pellets before film extrusion to avoid amorphous pellet sticking phenomenon.

From the dried pellets, films with a thickness of 400 μm were made using a LabTech LCR 300 film line. The coathanger die had a gap size of 1 mm, and the roll temperature was set to 65 °C. The extruder had an Ø 25 mm, 30 L/ᴅ screw, and the zone temperatures were set to 175–190 °C (from hopper to die). The rotational speed of the screw was 54 1/min, and the pulling peripheral speed was 1.0 m/min. Films were finally left to cool to room temperature of 22–24 °C. The specimens used for the research were obtained from the middle part of the films. Dumbbell-shaped specimens (ISO 527–3/4) and 60×60 mm flat specimens were cut from the films for the tensile tests and the ball burst tests, respectively.

Methods

Differential scanning calorimetry (DSC) measurements were made using a TA Instruments Q2000 DSC for the research. 4–5 mg small samples were investigated using nitrogen as purge gas at 50 mL min^{-1}. Non-isothermal scans were applied with a heating and cooling rate of 5 °C min^{-1} from 0 to 200 °C, to obtain the glass transition temperature (T_g), the cold crystallization temperature (T_{cc}), the enthalpy of cold crystallization (ΔH_{cc}), the melting temperature (T_m), the enthalpy of fusion (ΔH_m) from the heating scan and the crystallization temperature (T_c), and the enthalpy of crystallization (ΔH_c) from the cooling scan.

Crystallinity was calculated from the first heating scan to be able to investigate the effect of processing (1):

$$X = \frac{\Delta H_m - \Delta H_{cc}}{\Delta H_f(1 - \alpha)} \cdot 100 [\%], \tag{1}$$

where X [%] is the crystallinity, ΔH_m [J g^{-1}] and ΔH_{cc} [J g^{-1}] are the enthalpy of fusion and cold crystallization, respectively, while ΔH_f [J g^{-1}] is the enthalpy of fusion for the theoretically 100% crystalline PLA (93.0 J g^{-1}) [44] and α [−] is the mass fraction of the NR used.

A Zwick Z250 universal tensile tester (Ulm, Germany) was applied to the tensile testing of the PLA- and NR-filled PLA films cut in flow-wise ("production") direction (ISO 527–3/4 standard specimens) (Fig. 1).

Measurements were carried out at room temperature and on temperatures according to the thermoforming temperature of PLA (65 °C, 70 °C and 75 °C) using a heated chamber. Cross-head speeds of 50, 100, 200, 350 and 500 mm min^{-1} were used. The initial grip length was 115 mm, and the maximum grip length was 320 mm due to the geometric

Fig. 1 The measurement setup used for the tensile testing

limitations of the heat chamber. At elevated temperature, no specimens broke until reaching this maximum grip length; thus, for all of the specimens the drawn ratio was 1.78 (178%). After the tensile testing, the specimens were removed from the heated chamber to avoid further crystallization. All temperature and cross-head speed combinations were measured, and five parallel measurements were made.

A Zwick Z250 universal tensile tester was applied to perform ball burst tests. The apparatus was also used in our previous publication, where the detailed construction could be observed [43]. As a preparation for performing the measurement, the clamping ring is opened and then the disk specimen could be placed. The specimen is mounted by the sample fastener screw, and after controlling temperature, the measurement could be initiated. During the ball burst test, the ball moves vertically and the force–displacement values are recorded (Fig. 2).

The clamping fixture had a diameter of 54 mm, the inner hole had a diameter of 25 mm, while the diameter of the burst ball was 19 mm. Ball burst tests were performed at elevated temperatures of 65 °C, 70 °C and 75 °C. 50, 100, 200, 350 and 500 mm/min cross-head (ball burst) speed was applied on the specimens (60×60 mm samples cut from the films). We waited 5 min after placing the films into the heat chamber for reaching the desired temperature. The maximum burst extension was 65 mm due to the limits of this measurement. Neither of the specimens broke until this maximum extension was reached due to the elevated temperature testing and the specific force values were recorded at this extension. Even though ball burst tests better represent the multiaxial stress and strain conditions of thermoforming compared to the much simpler uniaxial tests; at the same time, it has its own limitations (limited strain rate of the tensile tester and limited maximum drawing height of the clamp design). Additionally, ball burst measurement as a testing method can only be applied to determine the force needed in the two major phases of thermoforming (heating and drawing), but it does not take the cooling and solidifying process into consideration. However, the mentioned heating and drawing phases are considered as the most important to predict how a plastic sheet can be thermoformed.

Results and discussion

Firstly, the first heating DSC curves (Fig. 3a and b) and the crystallinity values (Table 1) of the neat 2003D PLA and 2003D PLA + 10 mass% ENR films are investigated (both not tested (named as "reference") and tensile tested at lower and higher strain rates of 50 mm min^{-1} and at 500 mm min^{-1}, respectively).

On the first heating curve of the 2003D PLA reference, one can notice T_g (57.9 °C), T_{cc} (116.4 °C) and T_m
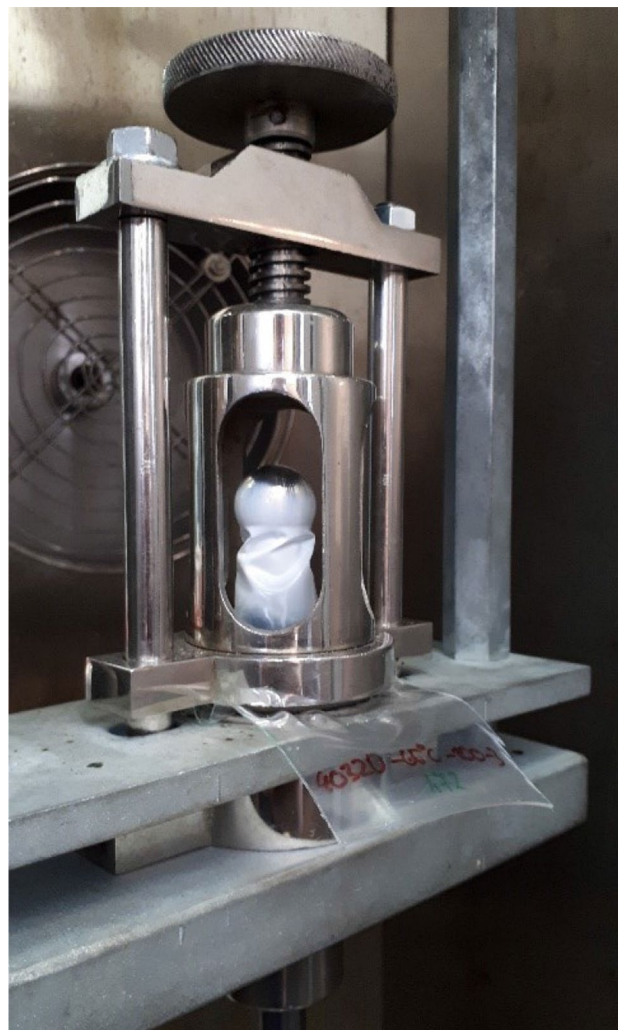
Fig. 2 The measurement setup used for the ball burst testing of the pure PLA and PLA + NR compound films

(148.8 °C). Since cold crystallization is visible on the curve, it proves that it was not possible for the crystallization to finish during cooling the extruded film. Crystallinity was found to be negligible, 1.7%, while crystal melt temperature also is rather low, which both are caused by the 4.3% D-Lactide content, which is considered as high. When 10 mass% ENR was added to the 2003D PLA grade, T_{cc} slightly decreased to 114.7 °C which presumes some, but insignificant nucleating effect. When the reference films are annealed (but not stretched), it only induced a slight increase in crystallinity. Please note that annealing time was selected as the same time as the tensile tested specimens took in the heated chamber. Accordingly, this time was not enough for significant crystallization, and thus, all the crystallinity increase in tensile tested specimens could be related to drawing caused orientation. When 2003D PLA and 2003D PLA + ENR compounds were tensile tested at 60 °C or 65 °C, crystallinity
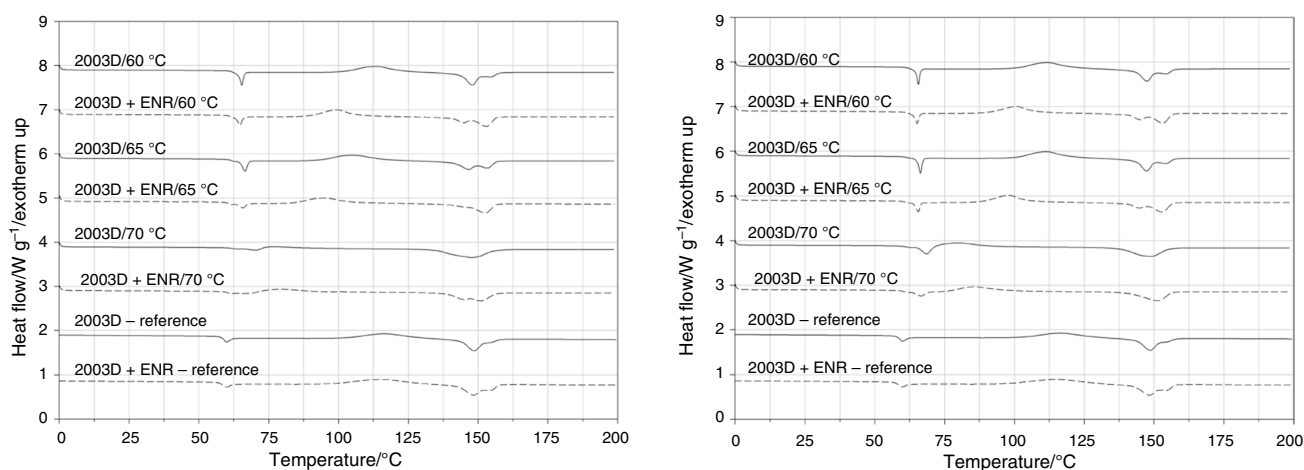
Fig. 3 First heating DSC curves of 2003D PLA and 2003D PLA + 10 mass% NR compound tensile tested at lower (50 mm min^{-1}) (**a**) and higher (500 mm min^{-1}) (**b**) cross-head speed and at various temperatures

Table 1 Crystallinity of 2003D PLA and 2003D PLA + 10 mass% NR films

Material/cross-head speed/mm min^{-1}	Tensile testing temperature		
	60 °C/%	65 °C/%	70 °C/%
PLA/50	1.0	0.4	29.9
PLA + 10ENR/50	2.3	0.6	23.2
PLA/500	1.8	2.1	16.8
PLA + 10ENR/500	1.9	1.0	11.9
PLA reference (annealed, not stretched)	0.3	0.5	1.7
PLA + 10 ENR reference (annealed, not stretched)	1.0	1.2	1.3
PLA reference (not annealed, not stretched)	0.2		
PLA + 10 ENR reference (not annealed, not stretched)	0.3		

still has not improved significantly even though drawing decreased the T_{cc} by 3–12 °C (50–500 mm min^{-1} drawing rate), while the presence of ENR decreased the T_{cc} by 14–20 °C (50–500 mm min^{-1} drawing rate). This represents that ENR had nucleating ability, but only in the case if the PLA + ENR films were drawn. At 70 °C drawing temperature, crystallinity highly improved due to the stretching, while below that temperature, the mobility of the molecular chains was not enough for folding and developing crystal phases. At 70 °C and 50 mm min^{-1} drawing rate, crystallinity of the neat PLA grade reached 29.9%, which was the entirely the effect of drawing alone; at the same time, when ENR was added to the compound, it retarded the crystallization and thus crystallinity was only found to be 23.2%. When native PLA was drawn at a higher rate (500 mm min^{-1}), it had lower crystallinity (16.8%) compared to the film that has been drawn at a lower strain rate of 50 mm min^{-1} (29.9%), because at this high drawing rate, molecular chains have much less time to fold and develop crystal phases or it is even possible that the high drawing rate causes the polymer chains to unfold and lamellae to slip. Again, when ENR was

added to PLA, crystallinity decreased from 16.8 to 11.9% at 70 °C and 500 mm min^{-1} drawing temperature and speed, respectively. According to the DSC curves of the drawn and pure PLA films, T_{cc} decreased so much that cold crystallization practically immediately begins right above T_g. This suggests that during drawing the PLA molecular chains are oriented, started to crystallize as a result, but supercooled at the end of the measurement (sample removed from heat chamber); thus, during the DSC measurement, when the sample gets enough heat and chain mobility, it instantly crystallizes, and also, in addition to the crystallinity, the ratio of the α and α' crystal forms also change when applying drawing. Additionally, ENR seems to have a double and contradictory effect on the crystallization of PLA. At the same time, it evidently decreases T_{cc} meaning that ENR particles help the appearance of PLA nuclei, which is considered as a nucleating ability; thus, ENR induces cold or melt crystallization. However, during drawing, ENR droplets may act as obstacles and eventually retard folding of the PLA chains; thus, ENR retards the drawing induced crystallization. Accordingly, ENR induces PLA crystallization, when

it is induced by heat, but retards the crystallization of PLA when it is induced by molecular folding and orientation. Finally, T_g also increased by 8–9 °C due to drawing, which widens the applicability of a such product.

Next, the first heating DSC curves (Fig. 4a and b) and the crystallinity values (Table 2) of the neat 4032D PLA and 4032D PLA + 10 mass% ENR films are investigated (both not tested (named as "reference") and tensile tested at low and high strain rates).

4032D has lower D-Lactide content (1.4%) compared to PLA grade 2003D (4.3%), which means faster crystallization and higher crystal melt temperature. Accordingly, the neat, reference 4032D PLA DSC curve had a T_g of 59.6 °C, a T_{cc} of 103.3 °C and a T_m of 168.8 °C. The T_{cc} decreased to 100.1 °C when 10 mass% ENR was added to PLA, which means again some minor nucleating ability. The crystallinity slightly increased due to annealing, but again, this annealing time was as not enough for significant crystallization, and thus, all the further crystallinity increase in tensile tested specimens could be related to drawing caused orientation. When the films were drawn at 50 mm min^{-1}, it

was found that crystallinity already significantly increased from 5.3 to 10.8% and 13.9% even using rather low drawing temperatures (60 °C and 65 °C). A possible explanation for this effect is the low D-Lactide content (and more isotactic structure) of 4032D PLA grade. When ENR was added to PLA, it even further increased the crystallinity of PLA and decreased the T_{cc} of the drawn films. The highest crystallinity values (30.5–42.9%) were reached again at 70 °C drawing, where ENR had minor influence. Similarly, to the 2003D PLA and 2003D PLA + ENR results, in case of the 4032D, the increasing drawing rate also retarded crystallization; at the same time, it was still possible to increase crystallinity using ENR for the high rate drawn films. Again, for the 70 °C drawn films (both neat PLA and PLA + ENR), when 50 mm min^{-1} drawing rate was used, the specimens almost fully crystallized during the drawing process, while for the 500 mm min^{-1} drawing rate, the specimens were not fully crystallized, but the T_{cc} was found right above T_g suggesting a supercooled state ready to instantly crystallize when chain mobility increases just above T_g. For the drawn films, in contrast to 2003D grade, NR induced crystallization
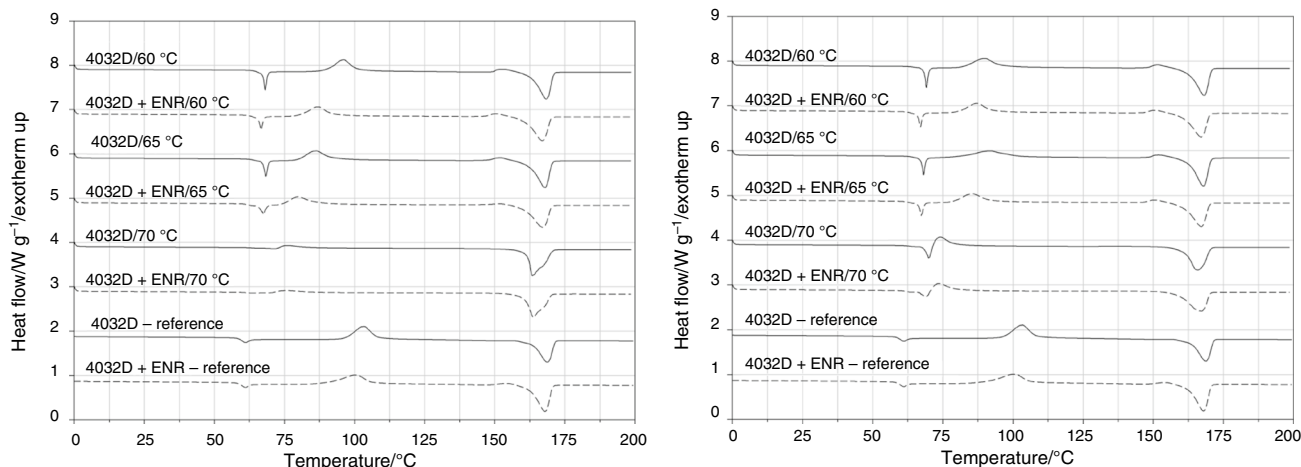
Fig. 4 First heating DSC curves of 4032D PLA and 4032D PLA + 10 mass% NR compound tensile tested at lower (50 mm min^{-1}) (**a**) and higher (500 mm min^{-1}) (**b**) cross-head speed and at various temperatures

Table 2 Crystallinity of 4032D PLA and 4032D PLA + 10 mass% NR films		Tensile testing temperature		
	Material/cross-head speed/mm min^{-1}	60 °C/%	65 °C/%	70 °C/%
	PLA/50	10.8	13.9	42.9
	PLA + 10ENR/50	16.8	25.0	42.0
	PLA/500	13.6	16.2	30.5
	PLA + 10ENR/500	17.1	17.2	32.4
	PLA reference (annealed, not stretched)	6.9	9.0	10.1
	PLA + 10 ENR reference (annealed, not stretched)	13.7	13.5	13.6
	PLA reference (not annealed, not stretched)	5.3		
	PLA + 10 ENR reference (not annealed, not stretched)	10.5		

for the 4032D grade. It seems that when NR was added to a rather slow crystallizing PLA, then it only retarded the crystallization of PLA; on the other hand, when NR was added to a faster crystallizing PLA grade, it could induce crystallization both due to nucleation and during drawing. Finally, T_g also increased by 8–10 °C when 500 mm min^{-1} high drawing rate was applied for the drawn 4032D PLA and 4032D PLA + NR films and this increase in T_g also suggests increase in heat deflection temperature. The effect of material parameters (D-Lactide content and NR content) as well as the testing parameters (drawing rate and temperature) on the crystallinity is summarized in Table 3.

There was no crystallinity measured for 4060D PLA and 4060D PLA + 10 mass% NR films independently from drawing rate or drawing temperature. This could be related to the atactic feature (high D-Lactide content) of 4060D PLA and thus its property to unable to crystallize.

The research was continued by the tensile test results (Figs. 5 and Fig. 6). First, the tensile strength of the films was investigated at room temperature (Fig. 5a).

As can be seen, the three different D-Lactide contents of PLA (and their compound with NR) had different behaviors. 4032D represented the highest, while 4060D the lowest strength values due to differences in crystallinity. The NR content evidently decreased the strength values since NR had lower own strength compared to PLA. Accordingly,

strength was measured as 52.9–71.6 MPa for native PLA grades, while 37.0–44.4 MPa for NR content PLA grades. Interestingly, by increasing cross-head speed, the curves have a saturation nature, with even a slight decrease in strength at high cross-head speeds. The curves increased when the drawing rate was increased (50–200 mm min^{-1}), which could be related to the general stiffening effect of viscoelastic materials [45]. At the same time, further increasing the drawing rate (200–500 mm min^{-1}) caused a saturation and even a slight reduction in strength for the PLA samples without NR content most probably caused by the mechanical energy input transformed into local warming of the samples. Moreover, the strength of 4060D PLA as an amorphous grade was found to be practically insensitive to changes in cross-head speed and also NR-filled PLA was found to be much less sensitive compared to the crystalline PLA grades without NR content. Overall, tensile strength was found to be dependent on four main factors including cross-head speed (stiffening effect), D-Lactide content of PLA used (crystallization behavior), potential local warming of the samples due to cross-head speed applied and the NR content (plasticizing effect and also crystallization modifier).

According to the elongation at break (Fig. 5b), it is difficult to find a distinct trend since the standard deviation was found quite high and thus the values could be considered as practically constants as a function of cross-head speed.

Table 3 The effect of various material and measurement parameters on the crystallinity

Material or measurement parameter	General effect on crystallinity
D-Lactide content	decreases
NR content	Dependent on D-Lactide content. Decreases for high D-Lactide content PLA, but increases for low D-Lactide content PLA
Drawing rate	decreases
Drawing temperature	increases
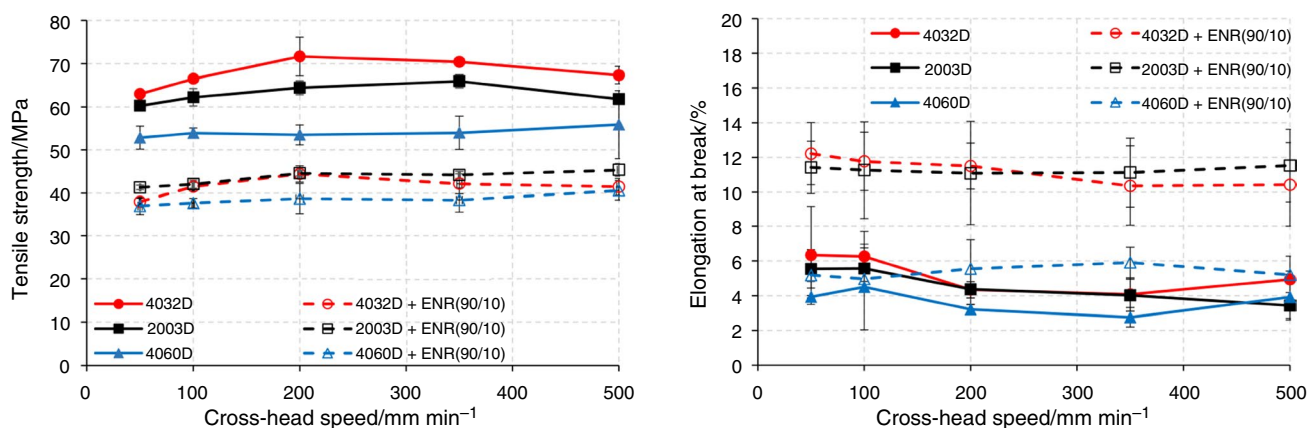
Fig. 5 Tensile strength (**a**) and elongation at break (**b**) of the 2003D, 4032D and 4060D pure PLA films as well as their compounds with 10 mass% NR content (room temperature measurement)
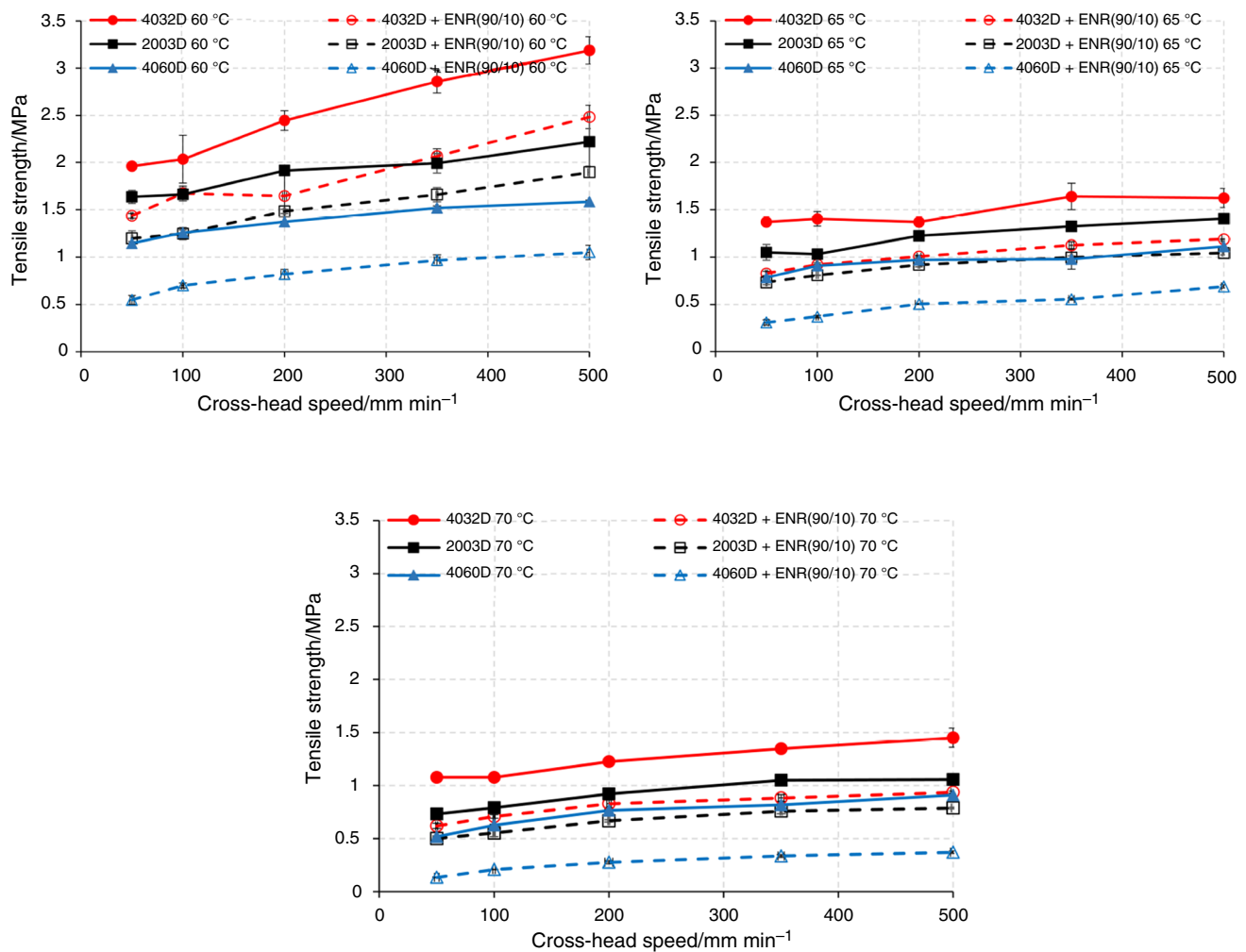
Fig. 6 Tensile strength of the 2003D, 4032D and 4060D pure PLA films as well as their compounds with 10 mass% NR content measured at 60 °C (**a**), 65 °C (**b**) and 70 °C (**c**)

Namely, for the native PLA films, it was between 2.75 and 6.33% with an average standard deviation of ± 1.1%. At the same time, apart from the high standard deviation, the average elongation at break values evidently reflected to the strength values discussed earlier and thus these two properties moved in the opposite direction. Thus, when strength increased (due to stiffening effect caused by increasing cross-head speed), elongation at break decreased, and when cross-head speed was further increased causing strength to decrease, elongation at break increased. In case of the NR-filled PLA films, elongation at break values could be considered as practically constant, which also reflects to the insensitivity of strength vales on the cross-head speed. Moreover, the elongation of the two semi-crystalline PLA grades significantly increased when adding NR, but for the amorphous grade (4060D), the addition of NR had minor effect, which highlights the influence of crystallinity, or in this case, the lack of crystallinity.

After tensile testing the films at room temperature, the next step was to investigate their properties using elevated temperatures of 60 °C, 65 °C and 70 °C (Fig. 6). Please note that at elevated temperature, the films were not broken during the measurements; thus, in this case not tensile strength but tensile stress is measured. The elongation of the films was restricted by the dimensions of the heat chamber applied; thus, the tensile measurements were stopped at a drawn ratio of 1.78 (178%) for all the measured films.

According to the tensile results measured at 60 °C, it was found that the tensile stress monotonously increased with increasing drawing rate all along with the investigated drawing rate range despite the decreased crystallinity found at higher drawing rates as demonstrated before. This suggests that the stiffening effect caused by increased drawing rate dominates the process. Additionally, it was found that the slope of the curves regarding the various PLA grades differs and thus their sensitivity for increasing

cross-head speed. 4032D film had a higher steepness of 0.0028 MPa $(\text{mm min}^{-1})^{-1}$, while 2003D and 4060D had 0.0013 MPa $(\text{mm min}^{-1})^{-1}$ and 0.0010 MPa $(\text{mm min}^{-1})^{-1}$, respectively. This could be related again to the difference in crystallinity, since at this temperature (60 °C), crystallinity of 4032D PLA films (with and without NR) was between 10.8 and 17.1%, while the crystallinity of 2003D PLA films was only between 1.0 and 2.3% (4060D was amorphous). It is worth to note that both materials had practically the same T_g of just a few °C lower compared to the testing temperature of 60 °C; thus, both were just in the rubbery state (the amorphous phase); accordingly, the crystal structure could still have significant effect in increasing the tensile stress with increasing cross-head speed. For NR-filled PLA films, all the curves represented lower stress values due to the soft phase of NR; at the same time, the order was the same; thus, 4032D + NR had the highest, while the amorphous 4060D + NR had the lowest stress values. Moreover, when increasing the testing temperature to 65 °C (Fig. 6b) or 70 °C (Fig. 6c), the stress values decreased even more.

The decrease in stress due to the increase in testing temperature is an expected consequence; however, the cross-head speed dependency also changed. In these cases of 65 °C and 70 °C testing temperature, all the curves had similar slope (between 0.005 and 0.009 MPa $(\text{mm min}^{-1})^{-1}$), meaning that differently to the behavior found at 60 °C testing temperature, this case the crystallinity alone was not enough to significantly increase the tensile stress. This could be explained that the testing temperatures applied are much more away from the T_g. Accordingly, the amorphous phase of PLA represented a much lower modulus (note that elongation during testing was the same for all the films) and thus the influence of crystalline structure decreased. The cross-head speed dependency without the effect of crystallinity could be investigated on the curves of 4060D amorphous PLA. The cross-head speed curve of this grade had practically the same slope as the other materials; thus, as it was pointed out before, crystalline structure had no significant effect at this testing temperature on cross-head speed dependency. At the same time, obviously, the higher the overall crystallinity
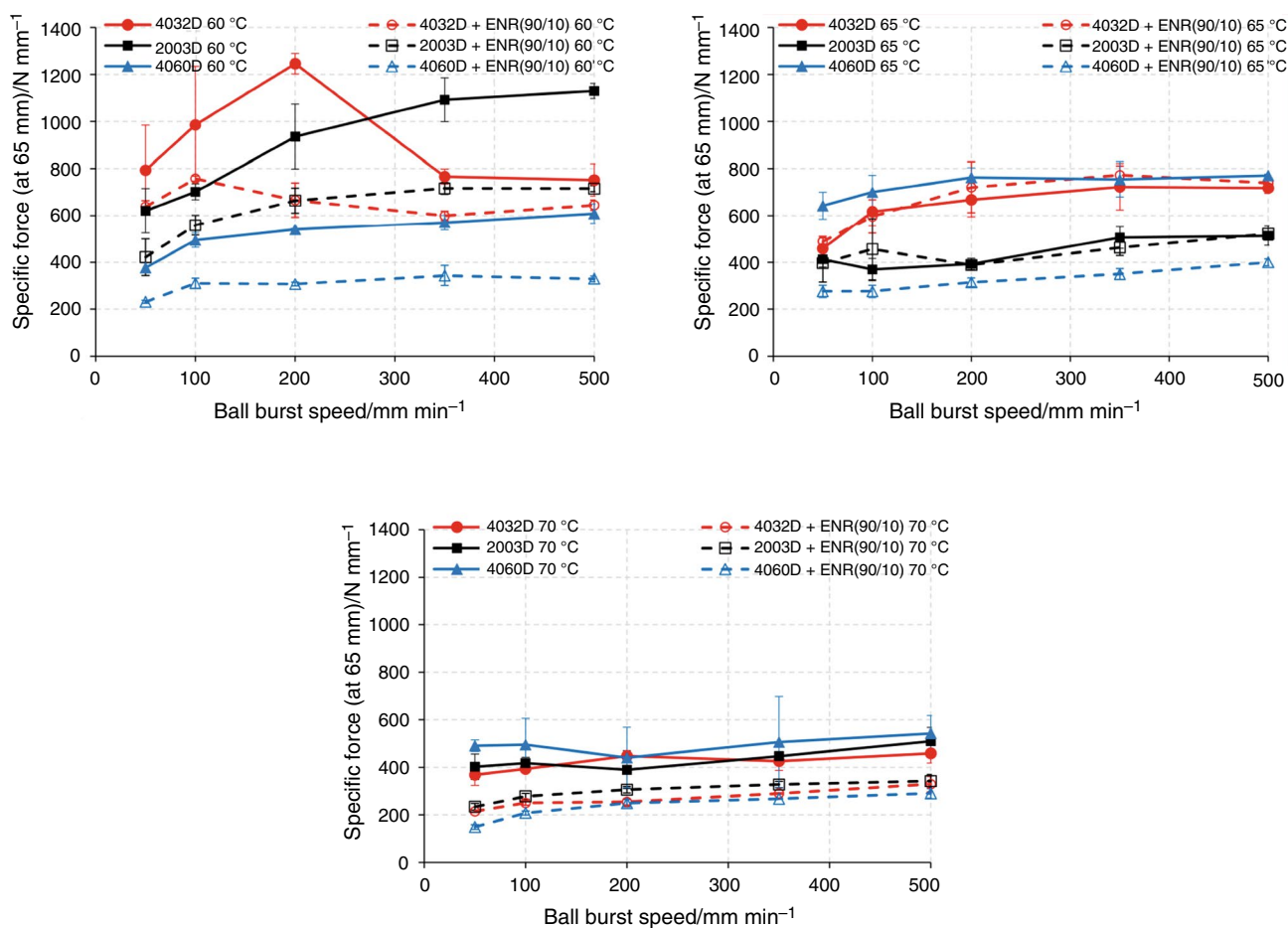
Fig. 7 Specific force of the 2003D, 4032D and 4060D pure PLA films as well as their compounds with 10 mass% NR content measured at 60 °C (**a**), 65 °C (**b**) and 70 °C (**c**)

was, the higher the tensile stress, but the cross-head speed dependency was found the same.

The research was continued by the ball burst tests (Fig. 7), which are closer to real thermoforming conditions then the tensile tests. Please note that in this case no room temperature test could be made, and during the test, a specific force was determined related to the maximum displacement of the ball clamp at 65 mm.

On the results of the ball burst tests (at 60 °C), some similarities and differences could be observed compared to the tensile tests performed at the same temperature. The similarities are that due to crystallinity, in most cases 4032D PLA sample had the highest, while 4060D PLA sample had the lowest specific force. Moreover, regarding the 2003D and 4060D PLA curves, they monotonously increased when ball burst speed was increased; additionally, in every case the addition of NR caused the specific force to decrease. Finally, the slope of the curves regarding the various PLA grades found to differ and thus their sensitivity for increasing ball burst speed. Besides these similarities, according to the 4032D PLA and 4032D PLA + NR curves, some major differences could be found. This is most probably related to the fact that applying ball burst test introduces a complex stress state that even more induces crystallization and then a single-axis tensile test and also introduces much higher mechanical energy input that could be transformed into local warming of the samples. Accordingly, the specific force curve of the 4032D PLA and 4032D PLA + NR was not monotonously increasing with increasing ball burst speed all along the investigated ball burst speed range, but there was a significant drop found above 200 mm min^{-1} and 100 mm min^{-1} for the PLA and for the PLA + NR samples, respectively. This suggests that in this case, the decreasing crystallinity (mechanical energy input transformed into local warming) found at higher drawing rates dominates the process instead of the general stiffening effect caused by increased drawing rate. At this testing temperature of 60 °C, the T_g of 4032D PLA is very near; thus, some additional heat introduced by high ball burst rates could highly decrease the modulus of the polymer causing decrease in specific force. When testing temperature was risen to 65 °C (Fig. 7b) or 70 °C (Fig. 7c), this phenomenon ceased, meaning that the curves were practically monotonously increasing taking the standard deviation of the measurements into consideration. 65 °C and 70 °C measurement temperatures were more away from T_g caused the curves to have similar slopes and the crystallinity to have less effect. Moreover, at these elevated temperatures, lower force was required for testing the samples. This was consistent with the previous tensile test results. It was finally found that despite the similar behavior of PLA films during elevated temperature tensile testing compared to ball burst testing, but the latter better represented the thermoforming conditions and also some major differences in film drawing behavior were found.

Conclusions

In our research, the thermoformability of Poly(Lactic Acid) (PLA)- and Epoxidized Natural Rubber (ENR)-filled PLA/NR blends was investigated using elevated temperature tensile testing and ball burst tests. Three PLA grades of 4032D, 2003D and 4060D were used representing different crystallization abilities. After compounding (PLA and 10 mass% ENR) and film extrusion, the films were tested for thermoformability using elevated temperature tensile tests as well as ball burst tests at 60 °C, 65 °C and 70 °C using various testing rates, while the crystallinity of the samples was also determined. It was found that ENR had a double and contradictory effect on the crystallization of PLA. It evidently had nucleating ability; thus, ENR induced cold or melt crystallization, but at the same time, during drawing, ENR particles might act as obstacles retarding the drawing induced crystallization. This phenomenon was dependent on the D-Lactide content of the PLA grade used. During the elevated temperature tensile testing, it was demonstrated that NR-filled PLA films represented lower stress values due to the soft phase of NR compared to pure PLA films. Also it was found that the stiffening effect caused by increased drawing rate dominates the tensile testing process representing monotonously increasing tensile stress despite the lower crystallinity measured at high drawing rates. Additionally, the slope of the curves measured at 60 °C was different for the various PLA grades and thus their sensitivity for increasing cross-head speed, which could also be related to crystallinity, since testing temperature was only a few °C above glass transition temperature of PLA. The slope of the curves became similar at higher testing temperatures, since the mobility of the amorphous phase highly increased and the films became less sensitive to their crystallinity. Regarding the ball burst tests, similarities were found compared to tensile tests like the monotonously increasing force values with increasing ball burst speed and the different slope of the curves reflecting to the crystalline structure and thus the sensitivity for increasing ball burst speed. At the same time, some differences were also found for the lowest D-Lactide content PLA grade due to the fact that applying ball burst test introduces a complex stress state that even more induces crystallization then a single-axis tensile test. This difference was in the curve of 4032D PLA, where a significant drop was found above 200 mm min^{-1} and above 100 mm min^{-1} for the neat PLA- and NR-filled PLA samples. This drop could be related to the decreasing crystallinity (mechanical energy input transformed into local warming) found at higher drawing rates that dominates the process instead of

the general stiffening effect caused by increased drawing rate. At higher testing temperatures (65 °C and 70 °C,) this phenomenon was not present.

References

1. Flieger M, Kantorová M, Prell A, Řezanka T, Votruba J. Biodegradable plastics from renewable sources. Folia Microbiol. 2003;48(1):27–44. https://doi.org/10.1007/BF02931273.

2. Luyt AS. Are biodegradable polymers the solution to the world's environmental problems? Express Polym Lett. 2017;11(10):764. https://doi.org/10.3144/expresspolymlett.2017.73.

3. Yu L. Biodegradable polymer blends and composites from renewable resources. New Jersey: Wiley; 2009.

4. Pilla S. Handbook of bioplastics and biocomposites engineering applications. New Jersey: Wiley; 2011.

5. Antunes A, Luyt AS, Kasak P, Aljarod O, Hassan MK, Popelka A. Effect of plasma treatment on accelerated PLA degradation. Express Polym Lett. 2021;15(8):725–43. https://doi.org/10.3144/expresspolymlett.2021.60.

6. Auras R, Lim L-T, Selke SEM, Tsuji H. Poly(lactic acid): synthesis, structures, properties, processing, and applications. New Jersey: Wiley; 2010.

7. Tábi T, Wacha AF, Hajba S. Effect of D-lactide content of annealed poly(lactic acid) on its thermal, mechanical, heat deflection temperature, and creep properties. J Appl Polym Sci. 2019;136(8):47103. https://doi.org/10.1002/app.47103.

8. Saeidlou S, Huneault MA, Li H, Park CB. Poly(lactic acid) crystallization. Prog Polym Sci. 2012;37(12):1657–77. https://doi.org/10.1016/j.progpolymsci.2012.07.005.

9. Lim L-T, Auras R, Rubino M. Processing technologies for poly(lactic acid). Prog Polym Sci. 2008;33(8):820–52. https://doi.org/10.1016/j.progpolymsci.2008.05.004.

10. Tábi T, Pölöskei K. The effect of processing parameters and calcium-stearate on the ejection process of injection molded poly(lactic acid) products. Period Polytech Mech Eng. 2022;66(1):17–25. https://doi.org/10.3311/PPme.18246.

11. Siakeng R, Jawaid M, Asim M, Saba N, Sanjay MR, Siengchin S, et al. Alkali treated coir/pineapple leaf fibres reinforced PLA hybrid composites: evaluation of mechanical, morphological, thermal and physical properties. Express Polym Lett. 2020;14(8):717–30. https://doi.org/10.3144/expresspolymlett.2020.59.

12. Józó M, Cui L, Bocz K, Pukánszky B. Processing induced segregation in PLA/TPS blends: factors and consequences. Express Polym Lett. 2020;14(8):768–79. https://doi.org/10.3144/expresspolymlett.2020.63.

13. Silva APB, Montagna LS, Passador FR, Rezende MC, Lemes AP. Biodegradable nanocomposites based on PLA/PHBV blend reinforced with carbon nanotubes with potential for electrical and electromagnetic applications. Express Polym Lett. 2021;15(10):987–1003. https://doi.org/10.3144/expresspolymlett.2021.79.

14. Antunes A, Luyt AS, Popelka A, Mahmoud A, Aljarod O, Hassan MK, et al. Influence of accelerated weathering on the physical and structural properties of poly(lactic-acid)/poly(3-hydroxybutyrate-co-3-hydroxyvalerate) (PLA/PHBV) blends. Express Polym Lett. 2021;15(8):687–707. https://doi.org/10.3144/expresspolymlett.2021.58.

15. Pan P, Inoue Y. Polymorphism and isomorphism in biodegradable polyesters. Prog Polym Sci. 2009;34(7):605–40. https://doi.org/10.1016/j.progpolymsci.2009.01.003.

16. Hoogsteen W, Postema AR, Pennings AJ, Brinke GT, Zugenmaier P. Crystal structure, conformation and morphology of solution-spun poly(L-lactide) fibers. Macromolecules. 1990;23(2):634–42. https://doi.org/10.1021/ma00204a041.

17. Sasaki S, Asakura T. Helix distortion and crystal structure of the α-form of poly(L-lactide). Macromolecules. 2003;36(22):8385–90. https://doi.org/10.1021/ma0348674.

18. Zhang J, Duan Y, Sato H, Tsuji H, Noda I, Yan S, et al. Crystal modifications and thermal behavior of poly(L-lactic acid) revealed by infrared spectroscopy. Macromolecules. 2005;38(19):8012–21. https://doi.org/10.1021/ma051232r.

19. Zhang J, Tashiro K, Domb AJ, Tsuji H. Confirmation of disorder α form of poly(L-lactic acid) by the X-ray fiber pattern and polarized IR/Raman spectra measured for uniaxially-oriented samples. Macromol Symp. 2006;242(1):274–8. https://doi.org/10.1002/masy.200651038.

20. Cho T-Y, Strobl G. Temperature dependent variations in the lamellar structure of poly(L-lactide). Polymer. 2006;47(4):1036–43. https://doi.org/10.1016/j.polymer.2005.12.027.

21. Puiggali J, Ikada Y, Tsuji H, Cartier L, Okihara T, Lotz B. The frustrated structure of poly(L-lactide). Polymer. 2000;41(25):8921–30. https://doi.org/10.1016/S0032-3861(00)00235-4.

22. Sawai D, Takahashi K, Sasashige A, Kanamoto T, Hyon S-H. Preparation of oriented β-form poly(L-lactic acid) by solid-state

coextrusion: effect of extrusion variables. Macromolecules. 2003;36(10):3601–5. https://doi.org/10.1021/ma030050z.

23. Cartier L, Okihara T, Ikada Y, Tsuji H, Puiggali J, Lotz B. Epitaxial crystallization and crystalline polymorphism of polylactides. Polymer. 2000;41(25):8909–19. https://doi.org/10.1016/S0032-3861(00)00234-2.

24. Tsuji H. Poly(lactide) stereocomplexes: formation, structure, properties, degradation, and applications. Macromol Biosci. 2005;5(7):569–97. https://doi.org/10.1002/mabi.200500062.

25. Hortós M, Viñas M, Espino S, Bou JJ. Influence of temperature on high molecular weight poly(lactic acid) stereocomplex formation. Express Polym Lett. 2019;13(2):123–34. https://doi.org/10.3144/expresspolymlett.2019.12.

26. Tsuji H, Ikada Y. Stereocomplex formation between enantiomeric poly(lactic acids). 9. Stereocomplexation from the melt. Macromolecules. 1993;26(25):6918–26. https://doi.org/10.1021/ma00077a032.

27. Tábi T, Hajba S, Kovács JG. Effect of crystalline forms (α' and α) of poly(lactic acid) on its mechanical, thermo-mechanical, heat deflection temperature and creep properties. Eur Polym J. 2016;82:232–43. https://doi.org/10.1016/j.eurpolymj.2016.07.024.

28. Dick JS. Rubber technology: compounding and testing for performance. Munich: Hanser; 2020.

29. Rodgers B. Rubber compounding: chemistry and applications. Boca Raton: CRC Press; 2015.

30. Bitinis N, Verdejo R, Cassagnau P, Lopez-Manchado MA. Structure and properties of polylactide/natural rubber blends. Mater Chem Phys. 2011;129(3):823–31. https://doi.org/10.1016/j.matchemphys.2011.05.016.

31. Pongtanayut K, Thongpin C, Santawitee O. The effect of rubber on morphology, thermal properties and mechanical properties of PLA/NR and PLA/ENR blends. Energy Procedia. 2013;34:888–97. https://doi.org/10.1016/j.egypro.2013.06.826.

32. Zhang C, Wang W, Huang Y, Pan Y, Jiang L, Dan Y, et al. Thermal, mechanical and rheological properties of polylactide toughened by expoxidized natural rubber. Mater Des. 2013;45:198–205. https://doi.org/10.1016/j.matdes.2012.09.024.

33. Xu C, Yuan D, Fu L, Chen Y. Physical blend of PLA/NR with co-continuous phase structure: preparation, rheology property, mechanical properties and morphology. Polym Test. 2014;37:94–101. https://doi.org/10.1016/j.polymertesting.2014.05.005.

34. Yuan D, Xu C, Chen Z, Chen Y. Crosslinked bicontinuous biobased polylactide/natural rubber materials: super toughness, "net-like"-structure of NR phase and excellent interfacial adhesion. Polym Test. 2014;38:73–80. https://doi.org/10.1016/j.polymertesting.2014.07.004.

35. Yuan D, Chen K, Xu C, Chen Z, Chen Y. Crosslinked bicontinuous biobased PLA/NR blends via dynamic vulcanization using different curing systems. Carbohyd Polym. 2014;113:438–45. https://doi.org/10.1016/j.carbpol.2014.07.044.

36. Suksut B, Deeprasertkul C. Effect of nucleating agents on physical properties of poly(lactic acid) and its blend with natural rubber. J Polym Environ. 2011;19(1):288–96. https://doi.org/10.1007/s10924-010-0278-9.

37. Jaratrotkamjorn R, Khaokong C, Tanrattanakul V. Toughness enhancement of poly(lactic acid) by melt blending with natural rubber. J Appl Polym Sci. 2012;124(6):5027–36. https://doi.org/10.1002/app.35617.

38. Chen Y, Yuan D, Xu C. Dynamically vulcanized biobased polylactide/natural rubber blend material with continuous cross-linked rubber phase. ACS Appl Mater Interfaces. 2014;6(6):3811–6. https://doi.org/10.1021/am5004766.

39. Bitinis N, Fortunati E, Verdejo R, Bras J, Kenny JM, Torre L, et al. Poly(lactic acid)/natural rubber/cellulose nanocrystal bionanocomposites. Part II: properties evaluation. Carbohydr Polym. 2013;96(2):621–7. https://doi.org/10.1016/j.carbpol.2013.03.091.

40. Hajba S, Tábi T. Cross effect of natural rubber and annealing on the properties of poly(lactic acid). Period Polytech Mech Eng. 2019;63(4):270–7. https://doi.org/10.3311/PPme.12825.

41. Tseng HH, Lai FS, Lee CK. Pneumatic bursting characteristics of plastics films. Polym Eng Sci. 1993;33(8):504–12. https://doi.org/10.1002/pen.760330810.

42. Warby MK, Whiteman JR, Jiang W-G, Warwick P, Wright T. Finite element simulation of thermoforming processes for polymer sheets. Math Comput Simul. 2003;61(3–6):209–18. https://doi.org/10.1016/S0378-4754(02)00077-0.

43. Pölöskei K, Csézi G, Hajba S, Tábi T. Investigation of the thermoformability of various D-Lactide content poly(lactic acid) films by ball burst test. Polym Eng Sci. 2020;60(6):1266–77. https://doi.org/10.1002/pen.25378.

44. Turner JF, Riga A, O'Connor A, Zhang J, Collis J. Characterization of drawn and undrawn poly-L-lactide films by differential scanning calorimetry. J Therm Anal Calorim. 2004;75:257–68. https://doi.org/10.1023/B:JTAN.0000017347.08469.b1.

45. Siviour CR, Jordan JL. High strain rate mechanics of polymers: a review. J Dyn Behav Mater. 2016;2(1):15–32. https://doi.org/10.1007/s40870-016-0052-8.